Kainate receptor-mediated synaptic currents in cerebellar Golgi cells are not shaped by diffusion of glutamate

Ingrid Bureau*, Stéphane Dieudonné†, Françoise Coussen*, and Christophe Mulle*‡

*Centre Nationale de la Recherche Scientifique UMR 5091, Institut François Magendie, Bordeaux 33077, France; and †Centre Nationale de la Recherche Scientifique UMR 8544, Ecole Normale Supérieure, Paris 75005, France

We report the presence of kainate receptors (KARs) in cerebellar Golgi cells of wild-type but not GluR6-deficient mice. Parallel fiber stimulation activates KAR-mediated synaptic currents [KAR-excitatory postsynaptic currents (EPSCs)] of small amplitude. KAR-EPSCs greatly differ from synaptic currents mediated by α-amino-3-hydroxy-5-methylisoxazole-4-propionate (AMPA) receptors (AMPAR-EPSCs) at the same synapse. KAR-EPSCs display slow rise and decay time and summate in response to a train of stimulations. By using PDA, a low-affinity competitive antagonist and agents that modify the clearance of glutamate, we show that these properties cannot be explained by diffusion of glutamate outside of the synaptic cleft and activation of extrasynaptic KARs. These data suggest that the slow kinetic of KAR-EPSCs is due to intrinsic properties of KARs being localized at postsynaptic sites. The contrasting properties of KAR- and AMPAR-EPSCs in terms of kinetics and summation offer the possibility for a glutamatergic synapse to integrate excitatory inputs over two different time scales.

Kainate receptors (KARs) are ionotropic glutamate receptors. KARs are assembled from five subunits (GluR5–7, KA1–2) that can form homomeric and heteromeric receptors but do not coassemble with α-amino-3-hydroxy-5-methylisoxazole-4-propionate (AMPA) receptor (AMPAR) subunits (1, 2). AMPARs are located postsynaptically where they mediate fast synaptic transmission. The subcellular localization and the functional role of KARs, which remain unclear, could depend on several parameters such as KAR subtype, cell identity, or synaptic structure. KARs are thought to modulate synaptic transmission by acting at a presynaptic level in CA1 and CA3 pyramidal cells (3–8). KAR-mediated synaptic responses [KAR-excitatory postsynaptic currents (EPSCs)] can be evoked in CA3 pyramidal cells (9–11), CA1 interneurons (12, 13), basolateral amygdala (14), dorsal horn neurons (15), OFF-bipolar cells of the retina (16), and layer IV neurons from barrel cortex of neonatal rats (17). Where tested, KAR-EPSCs and AMPAR-EPSCs result from the stimulation of the same population of axons (12, 15, 17). The slow kinetic of KAR-EPSCs is intriguing because it is not consistent with the fast activation, deactivation, and desensitization kinetics described for recombinant KARs and for native KARs recorded in cultured neurons (reviewed in ref. 3). These properties of KAR-EPSCs could in theory be attributed to an extrasynaptic location of KARs that would be activated by glutamate diffusing outside of the synaptic cleft. However, in CA3 pyramidal cells, blocking glutamate uptake does not affect KAR-EPSCs (9, 10), arguing against this hypothesis.

KAR subunit genes are abundantly expressed in a cell-type-specific manner in the cerebellum. *In situ* hybridization studies have shown the presence of GluR6 and KA2 subunit mRNA in granule cells. GluR5 and GluR6 subunits have been found by reverse transcription (RT)-PCR analysis in cultured granule cells (18). GluR5 and KA1 subunit mRNA have been detected

in Purkinje cells and GluR7 mRNA in interneurons of the molecular layer (19). Finally, the presence of functional KARs has been demonstrated in Purkinje cells in cerebellar slice culture (20) and in cultured granule cells (21, 22), but their role in synaptic transmission has not been addressed.

In this study, we report the presence of functional GluR6-containing KARs in Golgi cells, a population of γ-aminobutyric acidergic interneurons located in the granular layer of the cerebellum. These KARs are synaptically activated by parallel fiber stimulation. KAR-EPSCs display a slow rise and decay time and summate in response to a train of stimulations, in contrast to AMPAR-EPSCs. At variance with what was observed in CA3 pyramidal cells (9, 10), we found that blocking glutamate uptake enhanced KAR-EPSCs. We thus designed experiments to understand the mode of activation of synaptic KARs in Golgi cells and to test whether the slow kinetic of KAR-EPSCs is due to activation of extrasynaptic KARs by glutamate diffusing out from the synaptic cleft.

Materials and Methods

Cerebellar slices (250-μm thick) were prepared according to previously described methods (23, 24) from 12- to 25-day-old mice. Experiments were performed at room temperature. The slice was continuously perfused with a physiological saline solution of the following composition: 125 mM NaCl, 2.5 mM KCl, 2 mM $CaCl_2$, 1 mM $MgCl_2$, 1.25 mM NaH_2PO_4, 26 mM $NaHCO_3$, and 25 mM glucose (pH 7.4 when bubbled with a mixture of 95% O_2 and 5% CO_2). The internal solution contained 140 mM CsCl, 2 mM $MgCl_2$, 1 mM $CaCl_2$, 10 mM EGTA, 10 mM Hepes, 2 mM Na_2-ATP (pH 7.3). For current-clamp recordings, the internal solution contained 120 mM potassium gluconate, 20 mM KCl, 10 mM Hepes, 10 mM EGTA, 2 mM $MgCl_2$ and 2 mM Na_2-ATP (pH 7.3).

Golgi cells were identified according to visual and electrophysiological criteria described in ref. 25, in the vermal part of the central and anterior lobes. Whole-cell patch-clamp recordings, stimulations, and analysis of the data were performed as described previously (26). Averaged data are presented as means $\pm$ SEM. Statistical differences between two sets of data were assessed with a Mann–Whitney U test and with a Wilcoxon test for paired values.

To collect the cytosolic content of the cell, a gentle negative pressure was applied in the recording pipette. RT was performed

at 50°C for 30 min with 8 μl of Golgi and granule cell cytoplasms (or corresponding buffers as control) or 2 μg of mRNA from mouse cerebellum, with 20 units of avian myeloblastosis virus reverse transcriptase (Roche Scientific) and with primers corresponding to each KAR subunit: GluR5, 5'-GTTGGAGTTC-CAAATCCCAAT-3'; GluR6, 5'-CACCCCCAGAGCACTG-GCCTCTTTGCT-3'; GluR7, 5'-TGCGACGCTCGCTGG-TAGCA-3'; KA1, 5'-TCTGGAGTTGGAACCTGACAAA-3'; and KA2, 5'-CACCAGTTCTTCTAACCGCAGC-3'. Resulting cDNA were amplified separately in two sets of PCR. A first round of PCR was performed for 30 cycles using 3 μl of reverse transcriptase product as template and 10 pmol of primers corresponding to each subunit: 30 sec at 94°C, then 30 sec at 50°C (for GluR6 and GluR7) or 58°C (for GluR5, KA1 and KA2), and finally 75 sec at 72°C. A second round of PCR was performed using 3 μl of the first PCR product as template for 40 cycles. Predicted size of the PCR products were 403 bp (GluR5), 274 bp (GluR6), 200 bp (GluR7), 377 bp (KA1), and 210 bp (KA2). GluR5 primers: forward, 5'-GCTACATCCTCCCTCAGAC-CTCCCC-3' and reverse, 5'-AGATTATGCAGCTATCAG-CAGGGC-3'; GluR6 primers: forward, 5'-TTCCTGAATC-CTCTCTCCCCT-3' and reverse, 5'-CACCAAATGCCTC-CCACTATC-3'; GluR7 primers: forward, 5'-TGGAAC-CCTACCGCTACTCG-3' and reverse, 5'-TGCGACG-CTCGCTGGTAGCA-3'; KA1 primers: forward, 5'-ATGC-CCCGTGTCTCTGCTCCT-3' and reverse, 5'-TCTGGAGTT-GGAACCTGACAAA-3'; and KA2 primers: forward, 5'-ATGCCGGCTGAGCTGCTGCTG-3' and reverse 5'-TGCA GCTCAAAGATGTC-3'.

Most salts and chemicals were obtained from Sigma. 2,3-dihydroxy-6-nitro-sulfamoylbenzo[*f*]quinoxaline (NBQX) and DL-AP-5 were purchased from Tocris Cookson (Bristol, U.K.). GYKI 53655 (LY300168) was a generous gift from Lilly Research Laboratories (Indianapolis).

Results

GluR6-KARs in Cerebellar Golgi Cells. We compared the sensitivity of Golgi cells to kainate, a nonselective agonist for both KARs and AMPARs, between wild-type and GluR6$^{-/-}$ mice (11). In the presence of picrotoxin (100 μM), DL-AP-5 (50 μM) and tetrodotoxin (500 nM), bath application of kainate (300 nM) evoked an inward current in wild-type (76 ± 10pA, $n = 5$) but not in GluR6$^{-/-}$ mice ($n = 4$) (Fig. 1*A*). At concentrations of 1 and 3 μM, kainate activated significantly larger inward currents in wild-type mice than in GluR6$^{-/-}$ mice. In addition, GYKI 53655 (50 μM), a noncompetitive antagonist of AMPARs (27–29), completely blocked currents activated by 3 μM kainate in GluR6$^{-/-}$ mice ($n = 4$), whereas it only blocked this current by 51 ± 4% in wild-type mice ($n = 5$). These results indicate the presence of functional KARs in Golgi cells. These KARs are selectively activated by low concentrations of kainate (<1 μM) and comprise the GluR6 subunit. We analyzed the presence of KAR subunit mRNA in Golgi cells by single-cell RT-PCR (Fig. 1*B*). In control experiments, all five subunits were detected on total RNA from mouse cerebellum. Single-cell RT-PCR experiments indicated that granule cells express GluR6 and KA2 subunits whereas Golgi cells express GluR5 and GluR6, but not GluR7, KA1, and KA2.

KAR-Mediated Synaptic Currents in Golgi Cells. In the presence of picrotoxin (100 μM) and DL-AP-5 (100 μM), stimulation of parallel fibers in the molecular layer of the cerebellum evoked large EPSCs (804 ± 71pA, $n = 35$) in Golgi cells (30). These EPSCs were blocked by 50 μM GYKI 53655 (96.8 ± 0.6%, $n = 20$) or by 100 μM GYKI 52466 (97.5 ± 0.3%, $n = 15$), indicating that they are largely mediated by the activation of AMPARs (Fig. 2*A*). Nevertheless, a single stimulation consistently evoked a GYKI-resistant EPSC of small amplitude (27.4 ± 3.0 pA, $n =$
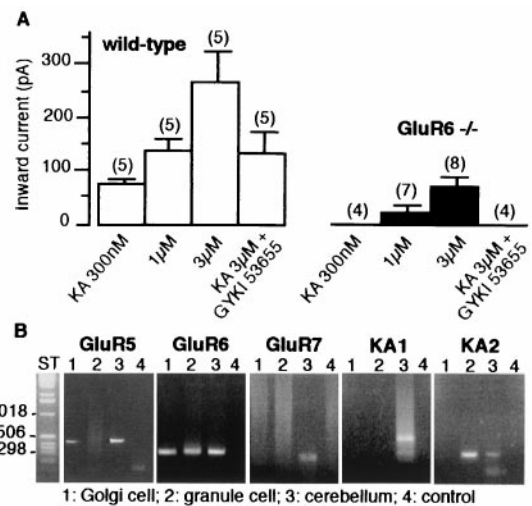

Fig. 1. KARs in Golgi cells. (*A*) Pooled data of the average amplitudes of inward currents activated by kainate in the presence and absence of GYKI 53655 (50 μM) in wild-type (□) and GluR6$^{-/-}$ (■) mice (mean ± SEM values; in parentheses, number of cell tested). Membrane holding potential was −70mV. All solutions were bath applied and contained tetrodotoxin (500 nM), D,L-AP-5 (50 μM), and picrotoxin (100 μM). (*B*) RT-PCR analysis of mRNA coding for kainate receptor subunits in Golgi cell (lane 1), granule cell (lane 2), total mouse cerebellum mRNA (lane 3), or pipette buffer as a control (lane 4). ST, one kb ladder.

34). This EPSC was blocked by 100 μM NBQX ($n = 5$), an AMPAR/KAR antagonist. In addition, GYKI 53655 and GYKI 52466 blocked EPSCs by >99% ($n = 9$ and $n = 7$, respectively;
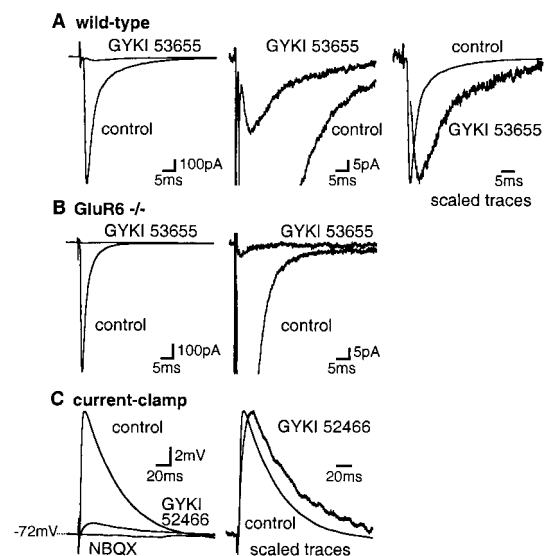
Fig. 2. Synaptic activation of KARs in Golgi cells by single stimulations. (*A*) (*Left*) EPSCs were largely blocked by GYKI 53655 (50 μM) in Golgi cells of wild-type mice. (*Middle*) Traces shown at an expanded amplitude scale. (*Right*) The GYKI-resistant EPSC is scaled to the peak of the control EPSC. Artifact was deleted from the trace of the GYKI-resistant EPSC. (*B*) (*Left*) In GluR6$^{-/-}$ mice, EPSCs were completely blocked by GYKI 53655 (50 μM). (*Right*) Traces shown at an expanded amplitude scale. (*C*) Current-clamp recordings. (*Left*) EPSPs were partially inhibited by GYKI 52466 (100 μM) and completely blocked by NBQX (100 μM). (*Right*) Traces shown at an expanded time scale. In this and the following figures, all solutions contained D,L-AP-5 (100 μM) and picrotoxin (100 μM). Each trace represents the average of 15–20 consecutive sweeps.
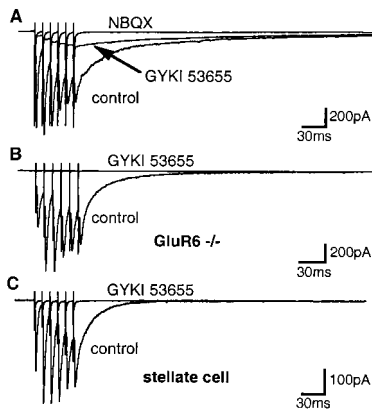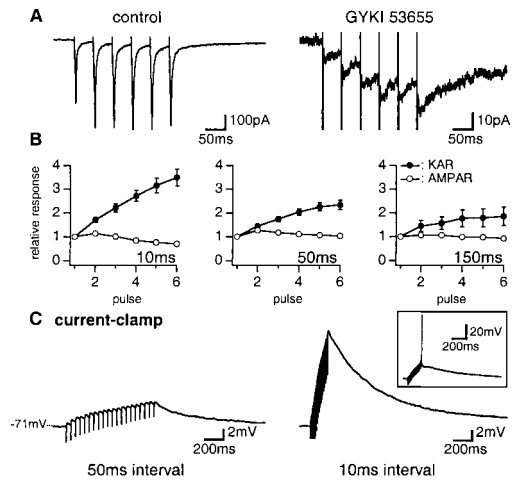
Fig. 3. Synaptic activation of KARs by repetitive stimulations. (*A*) Repetitive stimulations (100 Hz) evoked a slowly decaying compound EPSC partially inhibited by GYKI 53655 (50 μM) and completely blocked by NBQX (150 μM) in Golgi cells from wild-type mice. (*B*) In GluR6$^{-/-}$ mice, GYKI 53655 (50 μM) completely blocked the compound EPSC (*C*). GYKI 53655 (50 μM) completely blocked EPSCs evoked by train stimulations in stellate cell from wild-type mice.

Fig. 4. Summation of KAR-EPSCs during repetitive stimulations. (*A*) EPSCs evoked in Golgi cell by repetitive stimulations (50-ms interval) of parallel fibers in control conditions (*Left*) or in the presence of GYKI 53655 (50 μM) (*Right*). (*B*) Pooled data of the amplitude of AMPAR-EPSCs (○) measured in control conditions and KAR-EPSCs (●) measured in the presence of GYKI 53655 (50 μM) or GYKI 52466 (100 μM). The amplitude of EPSCs evoked by each pulse is measured in reference to initial baseline and is expressed as a function of the amplitude of the first pulse. Repetitive stimulations were performed with intervals of 10, 50, and 150 ms. (*C*) Current-clamp recordings. KAR-EPSPs evoked by repetitive stimulations with interval of 50 ms (*Left*) and 10 ms (*Right*) in the presence of GYKI 52466 (100 μM). In the *inset*, depolarization induced by summation of KAR-EPSPs reached the firing threshold.

different from wild-type with $P < 0.01$) (Fig. 2*B*) in Golgi cells from GluR6$^{-/-}$ mice. These results indicate that GYKI-resistant EPSCs were mediated by activation of GluR6-containing KARs at the parallel fiber-Golgi cell synapse. KAR-EPSCs displayed slow kinetics. The time to peak amplitude was 5.0 ± 0.3 ms for KAR-EPSCs ($n = 34$) and 3.4 ± 0.1 ms for AMPAR-EPSCs ($n = 31$) (values statistically different with $P < 0.001$) (Fig. 2*A*). The decay of KAR-EPSCs could be fitted by the sum of two exponentials with time constants $t1 = 12.3 \pm 3.1$ ms and $t2 = 62.6 \pm 8.5$ ms and a ratio of A2:A1 of 1.05 ± 0.21 ($n = 34$). AMPAR-EPSCs decayed much more rapidly with time constants of $t1 = 1.89 \pm 0.13$ ms and $t2 = 13.2 \pm 1.2$ ms and a ratio of A2:A1 of 0.26 ± 0.03 ($n = 31$) (Fig. 2*A*). The total charge carried by KAR-EPSCs represented $11 \pm 1\%$ (0.58 ± 0.09 pC, $n = 27$) of the total charges carried by the synaptic currents in control conditions (5.26 ± 0.45 pC, $n = 27$). In current-clamp recordings, parallel fiber stimulation evoked a small GYKI-resistant EPSP representing $9 \pm 5\%$ ($n = 5$) of the control AMPAR-EPSPs (Fig. 2*C*). The GYKI-resistant EPSPs displayed slower kinetics than AMPAR-EPSPs and were completely blocked by 100 μM NBQX, indicating that it was mediated by KARs (Fig. 2*C*).

Repetitive stimulation of parallel fibers (6 pulses, 10-ms interval) evoked compound synaptic currents that slowly decayed after the last stimulation (Fig. 3*A*). In the presence of GYKI 53655 (50 μM) or GYKI 52466 (100 μM), a slowly decaying compound EPSC persisted. This residual current was completely blocked by NBQX (50–150 μM) ($n = 10$) (Fig. 3*A*). The peak amplitude of the GYKI-resistant compound EPSC, referred to as compound KAR-EPSC, was 52.1 ± 9.8 pA ($n = 23$) in wild-type mice and 8.9 ± 1.4 pA ($n = 6$) in GluR6$^{-/-}$ mice (values statistically different with $P < 0.01$) (Fig. 3*B*). In wild-type mice, the charges carried by the compound KAR-EPSC (average value, 13.3 ± 2.2 pC, $n = 18$) represented 28% of the charges carried by the compound EPSC in control conditions. We tested the cell specificity of KAR-EPSCs by recording from stellate cells which are also innervated by parallel fibers. Stellate cells express GluR7 but not GluR6. In wild-type mice, single stimulation or train stimulation of parallel fibers evoked fast-decaying EPSCs in stellate cells which were completely inhibited by GYKI 53655 (50 μM) (Fig. 3*C*).

Summation of KAR-EPSCs During Repetitive Stimulations. We compared the properties of KAR-EPSCs and AMPAR-EPSCs dur-

ing repetitive stimulations at intervals of 10, 50, and 150 ms (Fig. 4). For an interval of 50 ms, the amplitude of AMPAR- and KAR-EPSCs evoked by the second stimulation was slightly larger as compared with the first one ($127 \pm 2\%$ and $110 \pm 3\%$, $n = 14$ and 23, respectively), an effect likely due to presynaptic paired-pulse facilitation. For all intervals tested, the amplitude of AMPAR- and KAR-EPSCs evoked by the following stimulations was constant (except for AMPAR-EPSCs evoked by train stimulations at 100 Hz, for which a decrease of amplitude was observed) (Fig. 4 *A* and *B*). We then measured the amplitude of the compound EPSC mediated by KARs and AMPARs after each successive stimulation within the train, taking the initial baseline as reference (see legend of Fig. 4*B*). In contrast with the compound AMPAR-EPSC, the amplitude of the compound KAR-EPSC increased with successive stimulations for all of these intervals (increase by a factor 3.5 ± 0.4, 2.3 ± 0.2 and 1.9 ± 0.4 for six stimulations at an interval of 10, 50, and 150 ms, $n = 13$, 23, and 8, respectively) (Fig. 4 *A* and *B*). It appeared that the compound KAR-EPSC was produced by the summation of successive EPSCs of constant amplitude. Temporal summation is made possible by the slow decay of KAR-EPSCs which do not return to baseline before the next stimulation. Apparent steady state is reached when the amplitude of each KAR-EPSC is balanced by the decay of the compound KAR-EPSC since the preceding stimulation. The summation of KAR responses was also observed in current-clamp recordings (Fig. 4*C*). By increasing the number and the frequency of stimulations within a train, membrane depolarization could reach the firing threshold (Fig. 4*C*).

Summation of KAR-EPSCs within a train could be due to low fractional occupancy of KARs allowing successive activation of additional pools of receptors at the same synapses. Alternatively, low probability of release at the parallel fiber-Golgi cell synapse could lead to the activation of different synapses at each pulse. If the probability of release was low, EPSCs would likely display
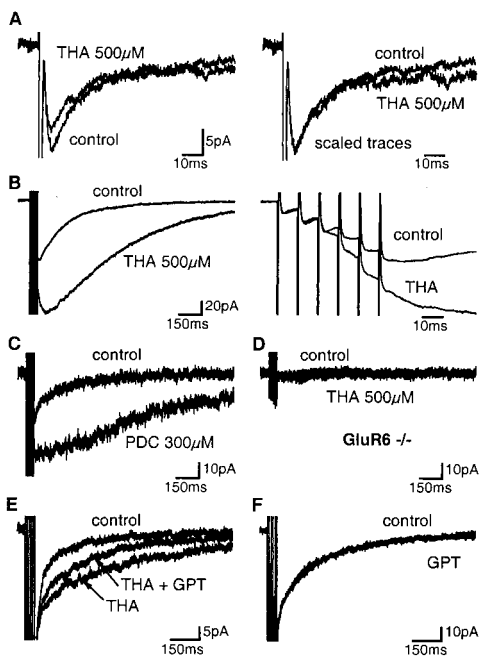
Fig. 5. Impact of the block of glutamate transporters on KAR-EPSCs. (*A*) (*Left*) THA (500 μM) had no effect on rise time and early phase of decay of single KAR-EPSCs. (*Right*) The EPSC evoked in the presence of THA is scaled to the peak of the control trace. (*B*) (*Left*) THA (500 μM) potentiated and prolonged compound KAR-EPSCs evoked by repetitive stimulations (6 pulses, 100 Hz). (*Right*) Traces shown at an expanded time scale. (*C*) PDC (300 μM) potentiated and prolonged compound KAR-EPSCs. (*D*) No additional current was observed during repetitive stimulations in the presence of THA (500 μM) in GluR6$^{-/-}$ mice. (*E*) GPT (5 units/ml) and pyruvate (2 mM) partially reversed the effect of THA (500 μM) on the decay rate of compound KAR-EPSCs evoked by repetitive stimulations. (*F*) GPT (5 units/ml) and pyruvate (2 mM) did not affect by itself the compound KAR-EPSCs in control conditions. All solutions contained GYKI 53655 (50 μM) or GYKI 52466 (100 μM).

a prominent paired-pulse facilitation and should be potentiated by increasing the extracellular Ca^{2+} concentration (31). As indicated above, paired-pulse facilitation of AMPAR- and KAR-EPSCs is modest (<30%). Furthermore, increasing the extracellular Ca^{2+} concentration to 3 mM while decreasing the Mg^{2+} concentration to 0.5 mM had no significant effect on the amplitude of single KAR-EPSCs (135 ± 34% of control, $n = 6$), and on the relative amplitude of each subsequent stimulation within a train (paired-pulse facilitation of 110 ± 11%, $n = 6$, not different from control conditions with $P > 0.3$). Thus, these data do not favor the hypothesis that summation of KAR-EPSCs is the result of the low probability of release at the parallel fiber-Golgi cell synapse.

Effects of Glutamate Transporter Blockers on KAR-EPSCs. Massive synaptic glutamate release followed by diffusion outside of the synaptic cleft may be able to raise the glutamate concentration in the surrounding extracellular space. The slow decay kinetic of KAR-EPSCs evoked by stimulation of fiber bundles may be shaped by the decay of the glutamate transient in the extracellular space. To test this hypothesis, we studied the impact on KAR-EPSCs of manipulations that modify glutamate clearance from the extracellular space. We first tested the effects of DL-threo-β-hydroxyaspartic acid (THA), a broad spectrum substrate/antagonist of glutamate transporters (32, 33), on KAR-EPSCs. In the presence of GYKI 53655 (50 μM) or GYKI 52466 (100 μM), THA (500 μM) decreased by 21 ± 4% the amplitude of single KAR-EPSCs ($n = 8$) (Fig. 5*A*). This effect may be due

to desensitization of KARs induced by the elevated resting concentration of glutamate in the whole extracellular space. THA did not change the rise time and the early phase of the decay of KAR-EPSCs (up to 30 ms). In contrast, we observed an increased synaptic current in the late phase of KAR-EPSCs (Fig. 5*A*). We compared the amount of charges carried during two sections of 20 ms each in the early and late phase of the KAR-EPSCs (the first starting from the peak and the second at 80 ms from the peak). In the presence of THA, the charges carried during the first and the second section were, respectively, 89 ± 5% and 143 ± 18% of the control (values statistically different with $P < 0.04$, $n = 8$).

The effects of THA (500 μM) were more pronounced on compound KAR-EPSCs (6 pulses, 100 Hz) (Fig. 5*B*). THA increased the peak amplitude of the compound KAR-EPSC in 9 of 15 cells tested. On average, the amplitude of compound KAR-EPSCs was potentiated by 1.5 ± 0.2-fold ($n = 15$). Closer inspection of the response revealed that the effect of THA was only observed after a delay of >20 ms (Fig. 5*B*). THA caused a large change in the kinetic of compound KAR-EPSCs. In 8 of 15 cells tested, compound KAR-EPSC reached its peak amplitude after a delay of 30 to 260 ms following the sixth pulse and then decayed to baseline. In all cells tested, the 20–80% decay time of the compound KAR-EPSCs increased by 3.1 ± 0.4-fold from 312 ± 37 ms in control conditions to 894 ± 124 ms in the presence of THA ($n = 15$). cis-2,3-piperidine-dicarboxylic acid (PDC; 300 μM), another blocker of glutamate transport, similarly increased the peak amplitude of the compound KAR-EPSCs by 1.5 ± 0.4-fold and prolonged the 20–80% decay time by 3.2 ± 0.7-fold ($n = 4$) (Fig. 5*C*). Synaptic currents recorded in the presence of THA were blocked by NBQX (100 μM) (data not shown) and were not observed in GluR6$^{-/-}$ mice (Fig. 5*D*), indicating that THA-dependent currents are due to the activation of GluR6-containing KARs. We also used an enzymatic scavenger to enhance the clearance of glutamate. Glutamic-pyruvic transaminase (GPT, alanine transaminase, EC 2.6.1.2) catalyses the conversion of glutamate and pyruvate to α-ketoglutarate and alanine. We compared the effect of THA on the decay time of KAR-EPSCs evoked by train stimulations (6 pulses, 100 Hz) before and during coincubation of GPT and pyruvate. GPT (5 units/ml) and pyruvate (2 mM) decreased the effect of THA (500 μM) on the 20–80% decay time of compound KAR-EPSCs by 32 ± 9% ($n = 5$, $P < 0.05$) (Fig. 5*E*). However, in control conditions, GPT and pyruvate did not affect the 20–80% decay time (104 ± 10% of control, $n = 5$) of compound KAR-EPSCs evoked by train stimulations (Fig. 5*F*).

Effects of Low-Affinity Competitive Antagonists on KAR-EPSCs. We used a low-affinity competitive antagonist (34) as an additional test for the activation of KARs located at extrasynaptic sites in control conditions. 2,3-cis-piperidine dicarboxylic acid (PDA) can be used to detect changes in glutamate concentration because the more glutamate is present, the more antagonist will be displaced by glutamate from receptors (35). If synaptically activated KARs were located at various distances from the synaptic cleft, then PDA should differentially affect the early and the late phase of KAR-EPSCs, because the concentration of glutamate decreases with distance. PDA at concentrations of 1 mM and 200 μM inhibited single KAR-EPSCs by 49 ± 5% and 8 ± 5%, respectively, but did not significantly modify the 20–80% decay time (94 ± 5% and 94 ± 10% of control, $n = 5$ and 7, respectively, $P > 0.3$) (Fig. 6 *A* and *B*). In the presence of PDA (1 mM), the charges carried during the early and late section of KAR-EPSCs were, respectively, 48 ± 7% and 59 ± 11% of the control (values not statistically different with $P > 0.2$, $n = 5$). In the presence of PDA (200 μM), these charges were, respectively, 86 ± 7% and 99 ± 30% of the control (values statistically not different with $P > 0.7$, $n = 7$). We tested the
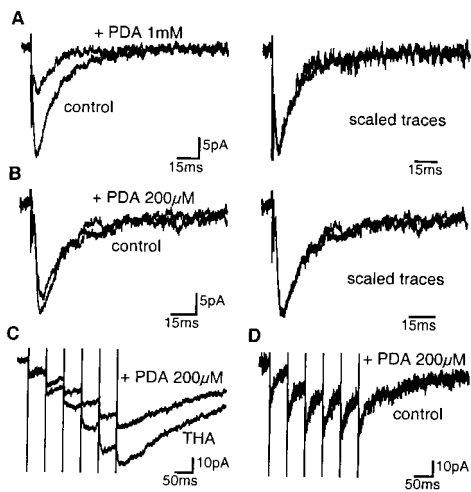
Fig. 6. KAR-EPSCs are not shaped by the build-up of glutamate concentration in the extracellular space. (*A*) (*Left*) the low-affinity competitive antagonist PDA (1 mM) partially blocked single KAR-EPSCs. (*Right*) The PDA-resistant KAR-EPSC is scaled to the peak of the control trace. (*B*) Same as in *A* with PDA (200 μM). (*C*) In the presence of THA (500 μM), PDA (200 μM) induced an increasing block of the successive KAR-EPSCs evoked by repetitive stimulations (6 pulse, 20 Hz). (*D*) In control conditions, PDA (200 μM) similarly affected successive KAR-EPSCs evoked by repetitive stimulations (6 pulses, 20 Hz). All solutions contained GYKI 53655 (50 μM) or GYKI 52466 (100 μM).

effects of PDA on compound KAR-EPSCs (6 pulses, 20 Hz) when glutamate transporters were blocked. In the presence of THA (500 μM), PDA (200 μM) more efficiently blocked the third than the first KAR-EPSC (37.5 ± 6.7% and 16.6 ± 4.7%, respectively, $n = 9$, values statistically different with $P < 0.04$) (Fig. 6*C*). This indicates that PDA inhibition is indeed sensitive to changes of glutamate concentration in the extracellular space. The increasing effect of PDA on KAR-EPSCs within a train of stimulations is probably due to the recruitment of extrasynaptic KARs activated by lower concentrations of glutamate diffusing in the extracellular space when glutamate uptake is blocked. However, in control conditions, no evidence for the activation of extrasynaptic KARs was observed in response to a train of stimulations. Indeed, in control conditions, PDA (200 μM) equally blocked the first and the third KAR-EPSCs (15.9 ± 5.8% and 15.3 ± 4.7%, respectively ($n = 7$) (Fig. 6*D*).

Discussion

In this study, we report the presence of KARs containing the GluR6 subunit in cerebellar Golgi cells. We demonstrate a role for GluR6-containing KARs in synaptic transmission at the parallel fiber-Golgi cell synapse. KAR-EPSCs differ in their time course and integration properties from AMPAR-EPSCs at the same synapse. We present evidence that these properties cannot be attributed to glutamate diffusion in the extracellular space and that synaptically activated KARs are localized at postsynaptic sites.

Functional KARs in Golgi Cells. *In situ* hybridization and immunocytochemistry studies have not provided evidence for an expression of KAR subunits in Golgi cells (19, 36). The hybridization signal for the GluR6 and KA2 subunits in these cells located in the granular layer can be masked by the intense labeling of granule cells. Using single-cell RT-PCR analysis, we demonstrate the presence of GluR6 and GluR5 mRNAs in the cytoplasm of Golgi cells. Low concentrations of kainate (<1 μM) evoked an inward current resistant to GYKI 53655, a selective AMPAR antagonist. The shift in the dose-response curve for the

amplitude of kainate-activated currents observed between wild-type and GluR6$^{-/-}$ mice confirms the presence of KARs in Golgi cells and provides evidence that these KARs comprise the GluR6 subunit.

EPSCs evoked by single stimulations of parallel fibers in Golgi cells are in large part mediated by activation of AMPARs. Nevertheless, in the presence of selective antagonists of AMPARs, stimulation of parallel fibers consistently evoked a synaptic current of low amplitude and slow rise and decay time. This synaptic current was blocked by high concentrations of NBQX and was absent in GluR6$^{-/-}$ mice. These results demonstrate a role for KARs at the parallel fiber-Golgi cell synapse and further define GluR6 as a component of these KARs.

KAR-EPSCs in Golgi Cells: Comparison to AMPAR-EPSCs. The amplitude of KAR-EPSCs only represented 3% of the amplitude of AMPAR-EPSCs at the same synapse. However, due to the large difference in their decay time, the relative charges carried by KAR-EPSCs represented >12% of the charges carried by AMPAR-EPSCs. KAR-EPSCs reported in other neuronal populations also display a slower rise and decay time than AMPAR-EPSCs (9, 12, 13, 15–17). The properties of AMPAR-EPSCs and KAR-EPSCs evoked by repetitive stimulations of parallel fibers, even at a moderate stimulation frequency (7 Hz), were also markedly different. In response to a short train of stimulations, the amplitude of the compound KAR-EPSC increased linearly after each successive stimulation. In contrast, the amplitude of the compound AMPAR-EPSC at the same synapse was constant after the second stimulation and tended to decrease at high stimulation frequencies. Overall, when comparing the synaptic response to a single stimulation and to a train of stimulations, charge transfer increased to a much larger degree for KAR-EPSCs than for AMPAR-EPSCs. In current-clamp recordings, temporal summation of KAR-EPSPs in response to a train of stimulation led to a large depolarization that could reach the firing threshold. Thus, at variance with AMPAR-EPSCs that mediate fast synaptic currents, KAR-EPSCs could serve to integrate synaptic currents in the 100-ms time scale. Several parameters are required for temporal summation to occur. The first parameter is the slow decay kinetic of KAR-EPSCs. In cerebellar Golgi cells, within a train of stimulation (frequency, 7–100 Hz) of parallel fibers, the subsequent stimulation takes place before the preceding KAR-EPSC has returned to baseline. The second parameter is the possibility to activate a new pool of KARs at each stimulation. Indeed, we show that the amplitude of each individual KAR-EPSC is constant within a train. There are two possible interpretations, either KARs are far from being saturated in response to a single stimulation or the probability of release at the parallel fiber-Golgi cell synapse is low, allowing activation of new sets of synapses in response to each consecutive stimulation. Our data are not in favor of the latter hypothesis. First, the paired-pulse facilitation ratio for both AMPARs and KARs is <30%. Then, the increasing extracellular Ca^{2+} concentration does not change the amplitude and the paired-pulse facilitation ratio of KAR-EPSCs. Finally, if a new set of synapses were activated in response to each consecutive stimulation, one would expect compound AMPAR-EPSCs to increase linearly when the interval between two stimulations within a train is shorter than the decay time (i.e., for intervals of 10 ms). Thus, our data favor the hypothesis that KARs are far from being saturated at the parallel fiber-Golgi cell synapse in response to a single stimulation. Further work is needed to evaluate the degree of saturation of KARs at this synapse.

Slow Decay of KAR-EPSCs Is Not Due to the Diffusion of Glutamate Out of the Synaptic Cleft. The slow kinetics and summation properties of KAR-EPSCs may either be due to intrinsic pharmacological

and biophysical properties of KARs or, alternatively, to an extrasynaptic localization of these receptors, as addressed by others (9, 10, 12). We have evaluated the impact of glutamate diffusion on KAR-EPSCs by the use of agents that modify the clearance of glutamate and by the use of a low-affinity competitive antagonist of KARs. If the slow rise and decay time of KAR-EPSCs were shaped by glutamate diffusing outside of the synaptic cleft, blocking glutamate transporters should affect the kinetics of KAR-EPSCs. THA, a blocker of glutamate transporters, did not affect the rise time and the early phase of decay of KAR-EPSCs. THA only affected the late phase of KAR-EPSCs, as described for AMPAR-EPSCs at mossy fiber/granule cell synapses (37). In addition, PDA, a low-affinity competitive antagonist, did not shorten the decay of KAR-EPSCs as would be expected if the slow decay time was due to the progressive activation of KARs located at various distances from the postsynaptic site, since the concentration of glutamate decreases away from the release site (38). Overall, these data strongly support the notion that diffusion of glutamate in extrasynaptic space cannot explain the slow rise and decay time of single KAR-EPSCs.

Extrasynaptic KARs might however be activated in response to a train of stimulations which yields summation of synaptic currents. We found that PDA inhibits to the same extent the first and the successive KAR-EPSCs within a train at 20 Hz. In addition, GPT, a glutamate scavenger, does not affect the time course of compound KAR-EPSCs, although we cannot exclude that this enzyme works too slowly to shape the concentration of glutamate released in control conditions. These results indicate that summation is not due to the build-up of glutamate in extracellular space. Thus, compound KAR-EPSCs result from the temporal summation of successive single KAR-EPSCs with similar properties. We found however that glutamate transporter blockers, THA and PDC, potentiated the amplitude of KAR-EPSCs evoked by repetitive stimulations. This potentiation was likely due to the activation of extrasynaptic KARs by glutamate diffusing outside from the synaptic cleft. Indeed, the effect of

THA on the decay of compound KAR-EPSCs was partially reversed by GPT. Furthermore, in the presence of THA, PDA (200 μM) induced an increasing block of successive KAR-EPSCs within a train of stimulations. Thus, when glutamate transport is blocked, repetitive stimulations allowed extrasynaptic KARs to be activated by lower concentrations of glutamate diffusing away from the synaptic cleft. In addition, these experiments validate the use of PDA as a sensor of changes in the concentration of glutamate-activating KARs. The lack of effect of PDC on KAR-EPSCs reported at the mossy fiber-CA3 pyramidal cell (9, 10) implies that, at this synapse, extrasynaptic KARs do not exist or that blocking glutamate uptake does not allow sufficient diffusion of glutamate to activate putative extrasynaptic KARs.

In control conditions, the slow kinetics of KAR-EPSCs in Golgi cells cannot be explained by glutamate diffusing away from the synaptic cleft. Extrasynaptic KARs (which might be located at neighboring synapses) can only be activated when glutamate transporters are blocked. The slow kinetics of KAR-EPSCs could be due to intrinsic properties of KARs being localized at postsynaptic sites. These properties of native synaptic KARs differ from those described for recombinant KARs (for review, see ref. 39) or for native KARs recorded from cultured neurons (40–42). This difference could involve the interaction of KARs with other unknown KAR subunits or with interacting proteins such as PSD-95 (43) or to the existence of an endogenous modulator. Alternatively, the slow kinetics of KAR-EPSCs could be due to a specific distribution of KARs in the synaptic cleft at more perisynaptic sites. The contrasting properties of KAR- and AMPAR-EPSCs in terms of kinetics and summation properties offer the possibility for a glutamatergic synapse to integrate excitatory inputs over two different time scales.

1. Bettler, B. & Mulle, C. (1995) *Neuropharmacology* **34,** 123–139.
2. Hollmann, M. & Heinemann, S. (1994) *Annu. Rev. Neurosci.* **17,** 31–108.
3. Chittajallu, R., Braithwaite, S., Clarke, V. & Henley, J. (1999) *Trends Pharmacol. Sci.* **20,** 26–35.
4. Clarke, V. R., Ballyk, B. A., Hoo, K. H., Mandelzys, A., Pellizzari, A., Bath, C. P., Thomas, J., Sharpe, E. F., Davies, C. H., Ornstein, P. L., *et al.* (1997) *Nature (London)* **389,** 599–603.
5. Kamiya, H. & Ozawa, S. (1998) *J. Physiol. (London)* **509,** 833–846.
6. Malva, J. O., Ambrosio, A. F., Cunha, R. A., Ribeiro, J. A., Carvalho, A. P. & Carvalho, C. M. (1995) *Neurosci. Lett.* **185,** 83–86.
7. Rodriguez-Moreno, A., Herreras, O. & Lerma, J. (1997) *Neuron* **19,** 893–901.
8. Represa, A., Tremblay, E. & Ben-Ari, Y. (1987) *Neuroscience* **20,** 739–748.
9. Castillo, P. E., Malenka, R. C. & Nicoll, R. A. (1997) *Nature (London)* **388,** 182–186.
10. Vignes, M. & Collingridge, G. L. (1997) *Nature (London)* **388,** 179–182.
11. Mulle, C., Andreas, S., Pérez-Otaño, I., Dickinson-Anson, H., Castillo, P. E., Bureau, I., Maron, C., Gage, F. H., Mann, J. R., Bettler, B., *et al.* (1998) *Nature (London)* **392,** 601–604.
12. Frerking, M., Malenka, R. & Nicoll, R. (1998) *Nat. Neurosci.* **1,** 479–486.
13. Cossart, R., Esclapez, M., Hirsch, J., Bernard, C. & Ben-Ari, Y. (1998) *Nat. Neurosci.* **1,** 470–478.
14. Li, H. & Rogawski, M. A. (1998) *Neuropharmacology* **37,** 1279–1286.
15. Li, P., Wilding, T. J., Kim, S. J., Calejesan, A. A., Huettner, J. E. & Zhuo, M. (1999) *Nature (London)* **397,** 161–164.
16. DeVries, S. & Schwartz, E. (1999) *Nature (London)* **397,** 157–160.
17. Kidd, F. L. & Isaac, J. T. (1999) *Nature (London)* **400,** 569–573.
18. Belcher, S. M. & Howe, J. R. (1997) *Brain Res. Mol. Brain Res.* **52,** 130–138.
19. Wisden, W. & Seeburg, P. (1993) *J. Neurosci.* **13,** 3582–3598.
20. Renard, A., Crepel, F. & Audinat, E. (1995) *Neuropharmacology* **34,** 335–346.
21. Savidge, J. R., Bleakman, D. & Bristow, D. R. (1997) *J. Neurochem.* **69,** 1763–1766.
22. Pemberton, K. E., Belcher, S. M., Ripellino, J. A. & Howe, J. R. (1998) *J. Physiol. (London)* **510,** 401–420.
23. Llano, I. & Gerschenfeld, H. M. (1993) *J. Physiol. (London)* **468,** 177–200.
24. Bureau, I. & Mulle, C. (1998) *J. Physiol. (London)* **509,** 817–831.
25. Dieudonné, S. (1995) *Proc. Natl. Acad. Sci. USA* **92,** 1441–1445.
26. Bureau, I., Bischoff, S., Heinemann, S. F. & Mulle, C. (1999) *J. Neurosci.* **19,** 653–663.
27. Wilding, T. J. & Huettner, J. E. (1995) *Mol. Pharmacol.* **47,** 582–587.
28. Paternain, A., Morales, M. & Lerma, J. (1995) *Neuron* **14,** 185–189.
29. Bleakman, R., Schoepp, D. D., Ballyk, B., Bufton, H., Sharpe, E. F., Thomas, K., Ornstein, P. L. & Kamboj, R. K. (1996) *Mol. Pharmacol.* **49,** 581–585.
30. Dieudonné, S. (1998) *J. Physiol. (London)* **510,** 845–866.
31. Zucker, R. S. (1989) *Annu. Rev. Neurosci.* **12,** 13–31.
32. Balcar, V. J., Johnston, G. A. & Twitchin, B. (1977) *J. Neurochem.* **28,** 1145–1146.
33. Arriza, J. L., Fairman, W. A., Wadiche, J. I., Murdoch, G. H., Kavanaugh, M. P. & Amara, S. G. (1994) *J. Neurosci.* **14,** 5559–5569.
34. Clements, J., Lester, R., Tong, G., Jahr, C. & Westbrook, G. (1992) *Science* **258,** 1498–1501.
35. Tong, G. & Jahr, C. E. (1994) *Neuron* **13,** 1195–1203.
36. Petralia, R., Wang, Y. & Wenthold, R. (1994) *J. Comp. Neurol.* **349,** 85–110.
37. Overstreet, L. S., Kinney, G. A., Liu, Y. B., Billups, D. & Slater, N. T. (1999) *J. Neurosci.* **19,** 9663–9673.
38. Barbour, R. & Häusser, M. (1997) *Trends Neurosci.* **20,** 377–384.
39. Dingledine, R., Borges, K., Bowie, D. & Traynelis, S. (1999) *Pharmacol. Rev.* **51,** 7–61.
40. Wilding, T. & Huettner, J. (1997) *J. Neurosci.* **17,** 2713–2721.
41. Lerma, J., Paternain, A. V., Naranjo, J. R. & Mellstrom, B. (1993) *Proc. Natl. Acad. Sci. USA* **90,** 11688–11692.
42. Huettner, J. E. (1990) *Neuron* **5,** 255–266.
43. Garcia, E. P., Mehta, S., Blair, L. A., Wells, D. G., Shang, J., Fukushima, T., Fallon, J. R., Garner, C. C. & Marshall, J. (1998) *Neuron* **21,** 727–739.

NEUROBIOLOGY